



# CHORUS

This is the accepted manuscript made available via CHORUS. The article has been published as:

## Electronic and magnetic properties of electron-doped $V_{2}O_{5}$ and $NaV_{2}O_{5}$

Churna Bhandari and Walter R. L. Lambrecht

Phys. Rev. B **92**, 125133 — Published 17 September 2015

DOI: [10.1103/PhysRevB.92.125133](https://doi.org/10.1103/PhysRevB.92.125133)

# Electronic and magnetic properties of electron doped $V_2O_5$ and $NaV_2O_5$

Churna Bhandari and Walter R. L. Lambrecht

*Department of Physics, Case Western Reserve University, Cleveland, OH 44106-7079*

Because of its narrow split-off conduction band, doping of  $V_2O_5$  leads to interesting strongly correlated electrons. We study the effects of doping on  $V_2O_5$ 's electronic and magnetic properties, either by adding electrons compensated by an artificial homogeneous background, or a virtual crystal approximation (VCA), by changing the atomic number  $Z_V$ , so as to keep charge neutrality, or by explicitly introducing Na as a dopant. The former two are considered as a way to simulate injected charge by gating, the latter occurs in the vanadium bronze  $NaV_2O_5$ . We also simulate  $Na_{1-x}V_2O_5$  using a virtual crystal approximation by changing the atomic number  $10 \leq Z_{Na} \leq 11$ . The differences in band structure resulting from how the electrons added to the band are compensated by positive charge in the three models are compared. The electronic band structures are calculated using the quasi-particle self-consistent QSGW method including a lattice-polarization correction and the local spin density functional method with Hubbard- $U$  corrections (LSDA+ $U$ ). For  $NaV_2O_5$ , the half-filling leads to a splitting of the up and down spin lowest  $d_{xy}$  band. The spins are found to prefer an anti-ferromagnetic ordering along the chain direction. Other spin configurations are shown to have higher energy and the exchange interactions are extracted and compared with literature. The optical conductivities are calculated and compared with experiment. Similar results are found for simply doping the band compensated by a background or virtual crystal approximation. However, the position of the occupied bands depends on the method chosen for compensating the charge. The most realistic way to simulate gating in which the compensating charge is kept away from the  $V_2O_5$  layer is the VCA with varying  $Z_{Na}$ . The splitting between the up and down spin bands depends on the filling. We find that below a certain concentration of about 0.88 electrons per V, the FM arrangement becomes preferable over the anti-ferromagnetic one. The magnetic moments then gradually decrease as we lower the filling of the split-off band.

PACS numbers: 71.20.Ps, 73.21.-b

## I. INTRODUCTION

A unique feature of  $V_2O_5$ , a layered material with weak interlayer van der Waals bonding, is that its lowest conduction band is separated from the rest of the conduction bands by a gap of about 1 eV and has essentially one-dimensional dispersion. The origin and dispersion character of this split-off narrow band is closely related to the unique structure of  $V_2O_5$ , which consists of chains within each layer. As explained in detail in our recent paper<sup>1</sup> and elsewhere,<sup>2,3</sup> the split-off band corresponds to V  $d_{xy}$  orbitals, with  $xy$  in the plane of the layer, which do not have an anti-bonding interaction with the bridge oxygen linking the two chains. All other V- $d$  orbitals have anti-bonding interactions with O- $2p$  orbitals and thus lie at higher energy. In pure  $V_2O_5$  this circumstance is of little importance because the band is empty. However, as soon as we add electrons to this band by doping, interesting effects can be expected. That is the reason why in this paper we study doping of  $V_2O_5$ .

The doping of  $V_2O_5$  is expected to play a significant role in various of its existing and potential applications. These include catalysis,<sup>4,5</sup> Li-ion batteries,<sup>6,7</sup> electrochromic devices,<sup>8</sup> and electro-optical switching devices.<sup>9</sup> The catalytic properties in oxidation reactions are in part related to the vanadyl oxygens which are singly bonded to V. Removing this oxygen also dopes the lowest conduction band.<sup>10</sup> However, alkali intercalation also plays a role in certain catalytic activities.<sup>5</sup> Li and other alkaline metals can be intercalated in the structure, and

may find interesting ionic conduction channels in  $V_2O_5$  nanostructures but also dope the system with electrons. Nanostructuring of  $V_2O_5$  has been explored recently in designing new types of Li ion batteries. From a fundamental science point of view, alkali and alkaline-earth intercalated  $V_2O_5$ , in particular  $NaV_2O_5$  have attracted great attention as so-called ladder compounds,<sup>2,11</sup> as discussed in detail below.

In a usual semiconductor, doping is mostly viewed as facilitating the transport by adding mobile electrons or holes in an otherwise empty or filled band. However, even at fairly high doping levels, one usually considers the bands themselves as fixed. In other words, one adopts a rigid band model. This is not entirely correct, but the deviations from rigid band behavior are small. It is well known, for example, that electron-interaction effects reduce the band gap slightly when the band is filled degenerately up to a Fermi level.<sup>12-14</sup> Also, the Moss-Burstein effect<sup>15,16</sup> of band filling on the optical absorption are well known. However, in  $V_2O_5$ , the lowest split-off narrow conduction band may be expected to become strongly modified by doping since the doping can fill a sizable fraction of the band. We are then faced with a narrow band with strong on-site Coulomb interactions because of the  $d$  character of the band. This situation leads to strong correlations and possibly magnetic effects. In addition, new optical absorption channels between the partially filled V- $d$  lowest band and the higher empty  $d$ -bands in the infrared and visible are probably involved in the electro-chromic activity.

There are several possible routes to doping  $V_2O_5$ . The one mostly explored in the past is intercalation with alkali and alkaline earth ions. There have been several studies of  $V_2O_5$  doped with various alkali or alkaline metals and even noble metals such as: Li<sup>17</sup>, Cs<sup>17,18</sup>, Na<sup>19</sup>, K<sup>19</sup>, Ag<sup>20</sup>, Mg<sup>17</sup>, Ca<sup>17</sup>, and Ag<sup>21</sup>. These materials are called vanadium bronzes. Some of these dopants perturb the crystal structure significantly from its native layered structure. For example, as one increases the concentration of Li in  $V_2O_5$ , several phases form. However, we are here only interested in the cases where the layered structure stays intact, except that the intercalates may somewhat extend the distance between the layer. This is the case of  $\alpha'$ - $NaV_2O_5$ . This material is an example of a so-called quarter filled ladder compound as explained in the next paragraph.

In fact,  $NaV_2O_5$  corresponds to doping of 1 electron per two  $d_{xy}$  orbitals, so a quarter filling of the corresponding bands. Since only one of those bands is split off from the rest of the conduction band continuum, it means the split-off band is half filled. Furthermore, this band has dispersion essentially only along the chains. This is then a half-filled Hubbard chain, and thus we indeed expect interesting correlation effects and anti-ferromagnetic ordering.  $NaV_2O_5$  has indeed been reported by Carpy *et al.*<sup>22</sup> to have an anti-ferromagnetic susceptibility with a an estimated Néel temperature of  $T_N \approx 320 \pm 50$  K. Because of the one-dimensional character, the ordering is not perfect and is probably accompanied by significant spin fluctuations even at fairly low temperature.

At 34 K a phase transition has been found in  $\alpha'$ - $NaV_2O_5$  to an even more interesting state.<sup>11</sup> It was first thought to be a spin-Peierls (SP) transition. The spin-Peierls transition corresponds to the dimerization of an anti-ferromagnetic 1D Heisenberg ( $S = 1/2$ ) chain. It corresponds to the formation of a minimum energy or gap for the spin-wave excitations. A historical review on the subject can be found in Jacobs *et al.*<sup>23</sup> Theoretically, it arises in the context of finding the ground state and low energy excitations of one-dimensional spin systems. Important papers on this subject include Bonner and Fisher<sup>24</sup>, Bulaevski<sup>25</sup>, Haldane<sup>26,27</sup>. Experimentally, such transitions were first observed in organic systems,<sup>23</sup> and subsequently in  $CuGeO_3$ .<sup>28</sup> It was then reported to occur in  $\alpha'$ - $NaV_2O_5$  by Isobe and Ueda.<sup>11</sup> However, the spin Peierls model in  $\alpha'$ - $NaV_2O_5$  was based on the assumption of a separate  $V^{4+}$  ( $S = 1/2$ ) and  $V^{5+}$  ( $S = 0$ ) chain corresponding to a non-centrosymmetric orthorhombic crystal structure with two inequivalent V and 5 inequivalent O sites, as determined by Carpy *et al.*<sup>22</sup> The latter was found to be incorrect by more accurate structure determinations.<sup>2,29</sup> The structure, at least above the transition temperature was found to be centrosymmetric  $P_{mnn}$ , which is the same space group as pure  $V_2O_5$  and a single spin was argued to occupy each V-O-V “rung” in a quarter filled ladder compound is a sort of molecular state.

Because of this finding, the phase transition was then

argued to consist of a charge ordering (CO)<sup>30</sup>, or possibly a charge ordering followed immediately by a spin-Peierls transition.<sup>31</sup> In fact, the centrosymmetric  $P_{mnn}$  structure was found to be no longer stable at low temperature. For instance, nuclear magnetic resonance (NMR) measurements show that there are 2 inequivalent vanadium sites below  $T = 34$  K one electron being localized in the  $3d_{xy}$  state of one vanadium ( $S = 1/2$ ) and another being empty non-magnetic ( $S = 0$ ) in a rung which clearly implies that the  $NaV_2O_5$  undergoes to a charge ordering phase transition. In fact, similar charge ordering is also revealed by x-ray diffraction<sup>32</sup> and dielectric<sup>33</sup> studies. Although a low temperature structure was determined by Ludecke *et al.*<sup>32</sup>, there is still a controversy about the charge ordering whether it occurs in every vanadium ladder<sup>30</sup> or in every other ladder.<sup>34,35</sup> There also is still some controversy about the nature of the ground state of the electrons in the V-O-V rungs, for which different results are obtained within open-shell Hartree-Fock and configuration interaction based cluster models.<sup>34,36</sup> Such models assign an important contribution to the singly occupied  $O^{\text{bridge}}p_y$  orbital configurations, while DFT based models consider this orbital always doubly occupied.

In the present paper, however, we will not delve into the nature of the low-temperature phase but focus on the anti-ferromagnetic state above 34 K. Instead our focus is on different approaches to doping and their effect on the electronic band structure.

Experimentally, other approaches to doping or “reduction” of  $V_2O_5$  to a lower oxide exist. It is pretty easy to see that vanadyl oxygen vacancies would dope the split-off band. Vanadyl oxygens are the oxygens that are bonded to one V via a triple bond. Breaking the bonds of this oxygen to V would mainly lower the  $d_{3z^2-r^2}$  and  $d_{xz}$ ,  $d_{yz}$  orbitals but these lie well above the  $d_{xy}$  derived split-off band so its electrons will dope the split-off band without introducing levels below it. This type of doping leads to lower oxides if the vacancies order and has also been studied to some extent although their electronic structure has not been fully explored. Studies of oxygen vacancies in  $V_2O_5$  can be found in Scanlon *et al.*<sup>37</sup> and Xiao *et al.*<sup>10</sup>.

With the recent developments in fabricating ultra-thin films of only a few atomic layers thick, for example by exfoliation, as used in graphene and transition metal dichalcogenides, another way of controlled doping becomes possibly available. These are thin enough that gating by means of a control electrode on the back side of the substrate on which the thin-film material is placed allows one to inject a sizable fraction of electrons in the material. Other possibilities for applying a higher field to the layer include electrolytic double layers on the surface or possibly a scanning tunneling microscope tip. A doping of 1 electron per  $V_2O_5$  formula unit corresponds to  $5 \times 10^{14}$  e/cm<sup>2</sup>. This is large but possibly within reach for a thin enough layer. The main advantage of this approach would be that doping could be pursued continuously without at the same time introducing scattering

centers and disorder in the film itself. It is similar in that sense to the approach of delta-doping in semiconductor heterojunctions. It could also be used in conjunction with intercalation. For example one might envision placing an atomically thin mono- or few-layer  $V_2O_5$  sample on an alkali metal covered surface and then with a bias voltage reducing or enhancing the carrier concentration in the layer.

Our focus in this paper is to compare this situation with doping by means of intercalation. In order to simulate additional electrons in the layer, we need to maintain charge neutrality. We can do this in two ways, either by adding a corresponding compensating homogeneous background, or by a so-called virtual crystal approximation (VCA), in which we replace the V core charge by a fractional number. For example to add 0.1 e per V we would add 0.1 to the atomic number of V. The approach with homogeneous background means that the corresponding positive charge is in part situated in the interstitial region between the layers, but also in part in the layer itself. On the other hand, in the case of actual doping by alkali metals such as Na, the positive  $Na^+$  ions are also situated in the interstitial region but in a discretized rather than continuous manner. The Na indeed creates energy levels high in the conduction band and just donates electrons to the system. We found that the split-off bands have negligible contribution from the Na. However, Na also modifies the structure slightly. Mostly, it increases the  $c$ -lattice constant, or distance between the layers. We have previously studied how increasing the  $c$ -spacing between the layer affects the electronic structure in our study of monolayer  $V_2O_5$ . Thus our goals are to compare the different ways in which these different approaches to doping affect the band structure.

In particular we focus on the energy region of the split-off bands and the gap. To first approximation, what one expects is that for half-filling of this band it may become favorable to split the band into its spin-up and down parts and in other words create a magnetic moment if the Stoner criterion is satisfied. However, the question than becomes: does the material become ferromagnetic or anti-ferromagnetic and what is the preferred way of ordering the moments? This situation corresponds closely to that of  $NaV_2O_5$  in the anti-ferromagnetic phase. We thus examine it first and make contact with the previous studies of this material. Next we investigate to what extent a similar band splitting and magnetism occur for doping without Na but using the background approach or VCA. Finally, since the latter allows to add arbitrary density of additional electrons, we can study whether the the magnetic phases persists for lower electron doping concentrations. This could in principle also be done by using  $Na_xV_2O_5$  and in fact concentrations  $0.9 < x < 1$  have been explored experimentally. However, here we also want to consider even lower concentrations. We can again do this within a VCA by using  $Z = 11 - x$  for Na.

Although several previous studies of  $NaV_2O_5$  made use of the LSDA+ $U$  approach, *i.e.* local spin density ap-

proximation with Hubbard- $U$  corrections, the quasiparticle self-consistent QSGW approach, which we applied recently<sup>1</sup> to  $V_2O_5$ , has not yet been applied to this material and may offer new insights because it provides a parameter free and starting point independent approach to the quasiparticle excitations. Nonetheless, in order to obtain a suitable starting point which already includes the expected spin-splittings, we will use LSDA+ $U$ . We emphasize that the final result however, is independent of this starting point.

As in our previous work<sup>38</sup>, we find that QSGW significantly overestimates the band gap for  $V_2O_5$  which is attributed in most part due to the missing lattice polarization effect in the screened Coulomb interaction  $W$ . We therefore estimate the lattice polarization effect using published results on the LO-TO splittings in  $NaV_2O_5$ . Essentially, this leads to a strong reduction in the  $GW$  self-energy. As a result LSDA is actually remarkably accurate for  $V_2O_5$ . Still, we will show it is important to go beyond it to include the correlation effects in the split-off  $d$  bands. These are, in effect, the main focus of the paper.

The paper is organized as follows. In section II, we revisit the first principles approximations such as: LSDA+ $U$  and QSGW. The section III is split in several subsections. First, in Sec. III A we review the structure and our structural relaxation results. Next, in Sec. III B we focus on  $NaV_2O_5$ . In this section, we first discuss band structure at different computational levels, then the optical properties and finally the magnetic exchange interactions. In the next subsection III C we discuss alternative models for doping, such as the homogeneous background and virtual crystal approximation, and finally we apply these methods to varying doping levels. In section IV, we conclude this work.

## II. METHODOLOGY

The full potential linear muffin-tin orbital (FP-LMTO)<sup>39,40</sup> method is used to solve the density functional Kohn-Sham eigenvalue problem within the local density approximation (LDA)<sup>41,42</sup>, or the local spin density approximation (LSDA) with Hubbard  $U$  corrections (LSDA+ $U$ ) as well as the quasiparticle equation in the QSGW approximation. The implementations used are available in Refs.43 and 44. In the FP-LMTO method used,<sup>39</sup> the basis set is specified by two sets of parameters, the smoothing radii  $R_{sm}$  and decay lengths ( $\kappa$ ) of smoothed Hankel function envelope functions. For  $NaV_2O_5$  we include ( $spd$ ,  $spd$ ) for V, ( $spd$ ,  $sp$ ) for O and ( $sp$ ,  $s$ ) for Na atoms respectively. These indicate the angular momenta included for each  $\kappa$ . The envelope functions are augmented inside the spheres in terms of solutions of the Schrödinger equation and their energy derivative up to an augmentation cut-off of  $l_{max} = 4$ .

The Brillouin zone integration  $\mathbf{k}$ -point convergence and other convergence parameters of the method were

carefully tested in our previous work of  $V_2O_5$  and similar criteria were adopted here. Specifically, we use a  $2 \times 6 \times 6$  un-shifted mesh for the Brillouin zone of the standard unit cell, along with the tetrahedron method for the metallic cases in the LDA self-consistent charge convergence. A slightly coarser sampling  $1 \times 3 \times 3$  was adopted for the calculation of the  $\Sigma$  in  $GW$  but the latter is interpolated to the finer mesh or the  $\mathbf{k}$ -points along symmetry lines in plotting the  $GW$  bands. For the anti-ferromagnetic cell doubled in the  $b$ -direction, we use a correspondingly smaller number of  $\mathbf{k}$ -points,  $2 \times 4 \times 6$  in LDA and  $1 \times 2 \times 3$  for QSGW.

As already mentioned in the introduction, one expects that the half-filled narrow band may become spin-split. Therefore we need to include spin-polarization. In some cases, however, the LSDA functional is not sufficient to create the splitting. Therefore we use the LSDA+ $U$  method, which adds an orbital dependent stronger Coulomb interaction  $U$  to the  $d$ -states. The smallest possible  $U$  providing a splitting was used. In fact, for the anti-ferromagnetic case, or in case of background doping, a splitting of the bands already occurred within LSDA without need for adding  $U$ . We stress, however, that we use this only as a starting point for the QSGW calculations. The results or the latter are independent of the starting point and the  $GW$  self-energy in the end replaces the additional potentials from the LSDA+ $U$  in going beyond LSDA. The quasiparticle self-consistent QSGW method is described in detail elsewhere.<sup>45–47</sup> The implementation parameters used here are similar as in our previous study of the band structure of bulk and monolayer  $V_2O_5$ .<sup>1</sup>

As mentioned earlier, in order to simulate doping by gating, we wish to add electrons without adding specific dopants. To keep the system neutral we employ two different approaches, either add a homogeneous background ( $QB$ ) or we distribute the counter charge over the nuclei of the  $V_2O_5$ . Although, this is not the only possible choice, we only modify the atomic number  $Z_V$  of the vanadium atoms.

### III. RESULTS

#### A. Structure of $NaV_2O_5$

As already mentioned, there have been numerous studies of  $NaV_2O_5$  in particular to elucidate the low temperature phase. The first experimentally proposed structure<sup>22</sup> at room temperature has the non-centrosymmetric  $P_{2_1mn}$  space group with two vanadium and 5 oxygen inequivalent sites. However this structure was refuted by later experimental results. Instead a centrosymmetric structure<sup>2</sup> was found at room temperature. This crystal structure is orthorhombic with the  $P_{mnn}$  space group with 1 vanadium and 3 inequivalent oxygen sites as in pure  $V_2O_5$  crystal. The unit cell is shown in Fig.1 and contains two formula units or a total of 16

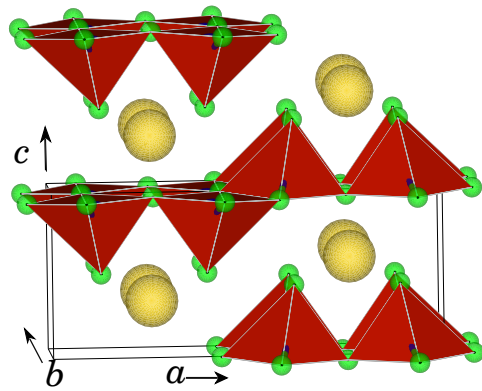


FIG. 1. (Color-online) Crystal structure of  $NaV_2O_5$  showing edge shared polyhedra alternatively pointing up and down. Here the blue spheres represent V, the yellow Na and the green O atoms respectively.

TABLE I. Bond lengths in  $\text{\AA}$ .

	V- $O_v$	V- $O_{cy}$	V- $O_{cx}$	V- $O_b$	Na- $O_b$	Na-V
Our	1.62	1.89	1.99	1.80	2.42	3.32
Expt. <sup>a</sup>	1.61	1.92	1.99	1.82	2.43	3.35

<sup>a</sup> By Smolinski *et al.*<sup>2</sup>

atoms: 2 Na, 4 V and 10 O atoms. The lattice constants are slightly changed from pure  $V_2O_5$ , for example  $a = 11.315 \text{ \AA}$  ( $11.512 \text{ \AA}$ ),<sup>48</sup>  $b = 3.61 \text{ \AA}$  ( $3.56 \text{ \AA}$ ), and  $c = 4.80 \text{ \AA}$  ( $4.37 \text{ \AA}$ ), where the numbers in parenthesis refer to pure  $V_2O_5$ . This amounts to  $-1.7\%$ ,  $1.4\%$  and  $9.8\%$  changes in  $a$ ,  $b$ ,  $c$  respectively. Clearly the  $c$  lattice constant increases the most. This also leads to a rotation of pyramids surrounding each V because the apical (vanadyl) oxygen anions are attracted towards the Na cation. This implies that some more intermixing of the different  $d$ -orbital types will occur.

We first carried out structural optimization in LDA for the  $NaV_2O_5$  case. To avoid the typical underestimate of experimental lattice constants in LDA, and the difficulties of standard density functionals to optimize the distance between Van der Waals bonded layers, we adopt the experimental lattice constants. Only the atomic internal coordinates were relaxed. The relaxation is carried out until the forces are less than  $10^{-3}$  Ryd/Bohr. As shown in Table I, the bond lengths of various atoms in  $NaV_2O_5$  slightly underestimate the experimental values. The bond lengths of Na to V or O correspond to nearest neighbor distances. Corresponding results for pure  $V_2O_5$  were reported in Ref.1.

#### B. Band structure of quarter-filled $NaV_2O_5$

We start our study with  $NaV_2O_5$ . First, we carried out non-spin-polarized (LDA) as well as spin-polarized (LSDA) and LSDA+ $U$  calculations for hypothetical

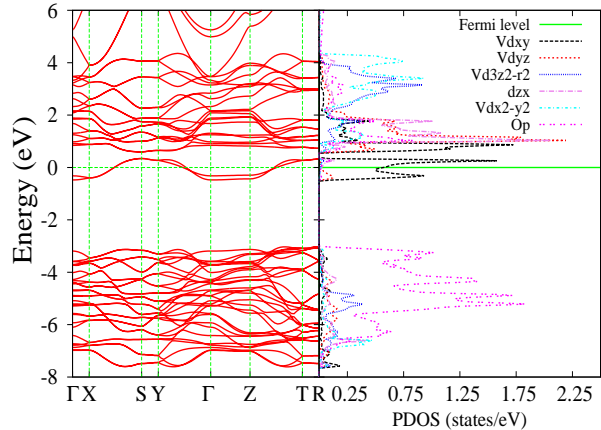


FIG. 2. (Color on-line) Non-spin-polarized LDA calculation of  $\text{NaV}_2\text{O}_5$  bands and density of states.

ferromagnetic (FM) and the actual anti-ferromagnetic (AFM) structure, which has alternating spin-up and spin-down along the chains in the  $b$  direction and parallel spins for V atoms in a bridge and for the two double chains occurring in the standard  $\text{V}_2\text{O}_5$  unit cell. Additional anti-ferromagnetic arrangements were also considered.

### 1. Non-spin-polarized band structure

The non-spin-polarized band structure and density of states is shown in Fig.2. As anticipated, the band structure looks very similar to that of pure  $\text{V}_2\text{O}_5$  with the difference that now the Fermi level is placed inside the split-off conduction band and is in fact precisely half-filled. The density of V- $d$  like states at the Fermi level  $D_{V-d}(\epsilon_F) = 0.657$  states/eV/spin and does not satisfy the Stoner criterion  $ID(\epsilon_F) > 1$  with the Stoner  $I = 0.354$  eV for vanadium taken from Janak.<sup>49</sup> Correspondingly, we indeed find that within LSDA, no magnetic moment forms and the band structure stays non-spin-polarized. However, within LSDA+ $U$  with a  $U_{\text{eff}} = U - J \approx 2.7$  eV and splitting of up and down spin states occurs and subsequently we can apply QSGW and find that formation of a magnetic moment persists. The value of  $U_{\text{eff}}$  is not critical. The value chosen here is chosen to mimic the results of the final QSGW as best as possible for the AFM case. The anti-ferromagnetic structure could in fact be stabilized even in LSDA without any  $U$ . As will be shown below the anti-ferromagnetic ordering of these moments along the  $b$  axis is preferred. However, before delving into the magnetic total energy differences, let us first discuss the band structure.

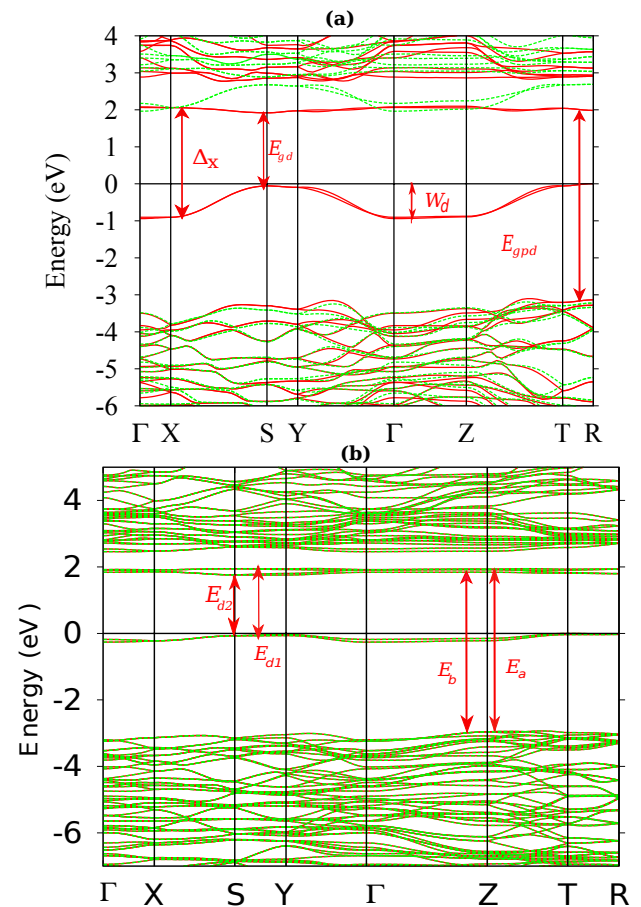


FIG. 3. (Color on-line) Band structures of  $\text{NaV}_2\text{O}_5$  obtained in the QSGW approach for (a) ferromagnetic and (b) anti-ferromagnetic ordering of the moments. Red solid lines indicate majority spin and green dashed line minority spin bands.

### 2. QSGW band structures in AFM and FM cases

The QSGW bands of FM and AFM  $\text{NaV}_2\text{O}_5$  are shown in Fig.3. As for pure  $\text{V}_2\text{O}_5$  we first notice a strong increase in the gap between O-2 $p$  valence bands and the bottom of the conduction bands (not counting the split-off band) to an unrealistic value of about 5 eV. This is even larger than in pure  $\text{V}_2\text{O}_5$  which results from the larger inter-layer distance or the increase in the  $c$  lattice constant by almost 10 %. We also see that the split-off band splits in up and down spin and the filled majority spin band is pushed down to about 2 eV below the continuum of  $d$ -conduction bands. One may recognize a corresponding minority spin band with almost identical dispersions. We call the more or less constant splitting between these two bands  $\Delta_x$ , the exchange splitting of the band. It is indicated in Fig.3 along with other splitting discussed later. Obviously in the LSDA+ $U$  approach, its value increases with the choice of  $U$  but it is not exactly equal to  $U$ . However, we also see a majority spin very flat band at 2 eV which is the second  $d_{xy}$  like band which has anti-bonding interactions with the bridge

oxygen but which is shifted down by the exchange interaction with the spin-polarization of the other  $d_{xy}$  band. In other words, the spin-polarization of the split-off band results in an induced spin splitting in all the higher lying  $d$ -bands. We can indeed see a splitting of up and down spin bands throughout the conduction band. In other words, we produced a ferromagnetic insulator instead of a metallic band structure. However, as will be discussed later, this is not the lowest energy structure because the spins prefer an AFM ordering along the chain.

Now, if we go to the AFM case, a similar gap structure occurs. There is a gap of about 3 eV between O-2*p* VBM and the lowest filled  $d$ -states. Then there is a gap of about 2 eV to the next empty states. A new set of 4 empty bands is split-off by about 0.4 eV from the continuum of  $d$ -bands. This is again the same splitting as we saw before for the FM bands and results from the induced spin-polarization in the higher  $d$ -bands. Remarkably, however, the dispersion of the filled split-off band is now strongly reduced. The band width of the FM split-off band was about 1 eV but in the AFM case it is reduced to only about 0.2 eV. This results from the fact that in a collinear spin calculation, hopping only occurs between orbitals of the same spin and so along the chain direction, the nearest neighbor V hopping is now suppressed and only much weaker second nearest neighbor hopping contributes to the band width. If we examine this band structure as function of  $U_{\text{eff}}$  in LSDA+ $U$ , we find that the splitting between the first empty and first occupied  $d$  band stays more or less constant but the splitting between the filled  $d$  band and the empty  $d$  band continuum increases, so the filled band gets pushed closer to the O-2*p* bands. This is because the larger  $U$ , the more the occupied spin states are pushed down but the lowest separate set of empty bands are not the corresponding opposite spin bands but rather the  $d_{xy}$  bands that are anti-bonding with bridge O- $p_y$ .

### 3. QSGW with lattice polarization correction

The QSGW band structure in this material is quite unrealistic and as we proposed in Bhandari *et al.*<sup>1</sup> for pure  $V_2O_5$  which can be largely attributed to the importance of lattice polarization contributions to the screening of  $W$  in these materials. This results from the strong LO-TO splitting of the phonons. The LO phonons lead a contribution to the dielectric screening for long wavelengths ( $\mathbf{q} \rightarrow 0$  limit) which affects the screening of the electron-electron interaction even though the LO phonons are much lower frequency than the electronic inter-band transitions. The generalized Lyddane-Sachs-Teller relation gives this increase in the screening due to lattice polarization as:

$$\varepsilon_{\text{tot}}^\alpha(\mathbf{q} \rightarrow 0, \omega) = \varepsilon_{\text{el}}^\alpha(\mathbf{q} \rightarrow 0, \omega) \prod_i \frac{\omega_{LOi}^2 - \omega^2}{\omega_{TOi}^2 - (\omega + i0^+)^2}, \quad (1)$$

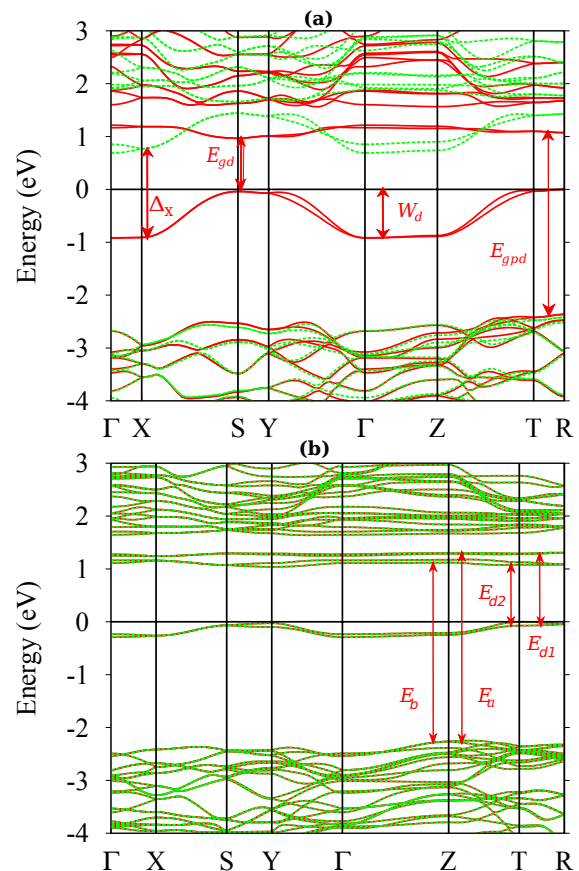


FIG. 4. (Color on-line) Band structures of  $\text{NaV}_2\text{O}_5$  obtained in the QSGW- $\alpha\Delta\Sigma$  approach with  $\alpha = 0.38$  for (a) ferromagnetic and (b) anti-ferromagnetic ordering of the moments.

where the product is over all modes corresponding to the irreducible representation to which the Cartesian component  $\alpha$  belongs. In practice, we estimate this effect by taking the  $\omega \rightarrow 0$  limit and assuming that the  $GW$  self-energy shift  $\Delta\Sigma$  is dominated by the static screened exchange contribution. Thus we multiply  $\Delta\Sigma$  by a reduction factor  $\alpha = \varepsilon_{\text{el}}/\varepsilon_{\text{tot}}$ . To take in to account the anisotropy we average over directions by multiplying the Cartesian components and taking the cube root. In pure  $V_2O_5$  this led to a reduction factor of  $\alpha = 0.38$ . In the present case, using phonons for  $\text{NaV}_2\text{O}_5$  as reported in Popova *et al.*<sup>50</sup> we obtain a reduction factor  $\alpha = 0.5$ . The phonons in  $V_2O_5$  and  $\text{NaV}_2\text{O}_5$  are indeed very similar and this difference should be considered to be within the uncertainty of the approach, which is only a crude way of estimating the lattice polarization effect to begin with. We thus keep the  $\alpha = 0.38$  as in our previous  $V_2O_5$  calculation for easier comparison.

The corresponding band structures are shown in Fig.4. The gap between the O-2*p* like VBM of  $V_2O_5$  and the lowest now filled V-3*d* band is about 1.81 eV and the gap between the filled  $d$  band (new VBM) and the empty  $d$  bands is now about 1-1.3 eV, slightly lower in the FM than in the AFM case. Also note that in the FM case,

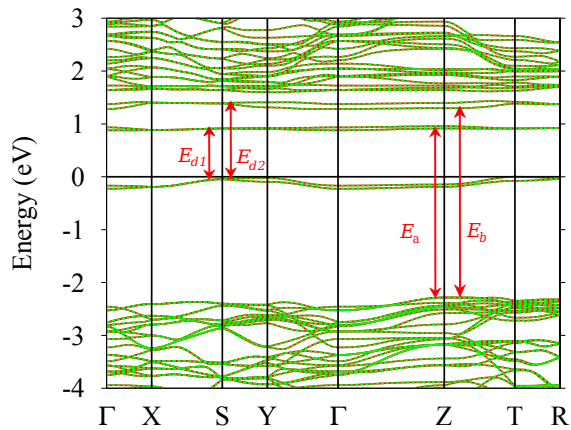


FIG. 5. (Color on-line) Band structure of AFM  $\text{NaV}_2\text{O}_5$  within LSDA+ $U$  with  $U_{\text{eff}} = 2.7$  eV.

the lowest gap is indirect between the majority spin filled split-off band at  $S$  and the corresponding minority spin band at  $\Gamma$ . However, the lowest direct allowed transitions would be between the majority spin bands at  $S$ . The splitting between up and down spin  $d_{xy}$  bands is about 2 eV and is uniform throughout the Brillouin zone. This corresponds to the exchange splitting  $\Delta_x$  of these bands and justifies the previous use of a  $U_{\text{eff}} \approx 2.7$  eV in LSDA+ $U$ . In the AFM case this splitting cannot be so easily identified and the gap between lowest filled and lowest empty  $d$  band is slightly larger, about 1.3 eV.

There are further small differences between LSDA+ $U$  and these  $0.38\Delta\Sigma$  QSGW results. Overall, similar band structures to ours were obtained by Ming *et al.* using LSDA+ $U$ .<sup>51</sup> We include in Fig.5 our band structure within LSDA+ $U$  with  $U_{\text{eff}} = 2.7$  eV because it agrees best with optical response as will be shown in the next subsection. In particular, we may note a slightly larger splitting of the two sets of empty split-off  $d$ -bands below the continuum of the conduction band.

#### 4. Optical response

We now compare these results with experimental data of the optical conductivity by Konstantinovič *et al.*<sup>52</sup> Similar results were obtained by Atzkern *et al.*<sup>53</sup> from electron energy loss spectroscopy (EELS) and by Presura *et al.* by spectroscopic ellipsometry.<sup>54</sup> To this end we calculate the optical conductivity for  $\mathbf{E} \parallel \mathbf{a}$  and  $\mathbf{E} \parallel \mathbf{b}$ , as shown in Fig.6. We compare both the LSDA+ $U$  with  $U = 2.72$  eV and the  $0.38\Delta\Sigma$  QSGW with experiments.

Experimentally, a peak in optical conductivity is found at about 1 eV for  $\mathbf{E} \parallel \mathbf{a}$  and assigned to transitions between the highest filled and lowest empty V- $d$  states.<sup>52</sup> This agrees well with our calculation, which shows a strong peak at about 1 eV in LSDA+ $U$  case but in the  $0.38\Delta\Sigma$ -QSGW case this peak is found a little higher at 1.5 eV. Further inspection of the PDOS (in LSDA+ $U$ ) shown in Fig.7 shows that this corresponds to a transition

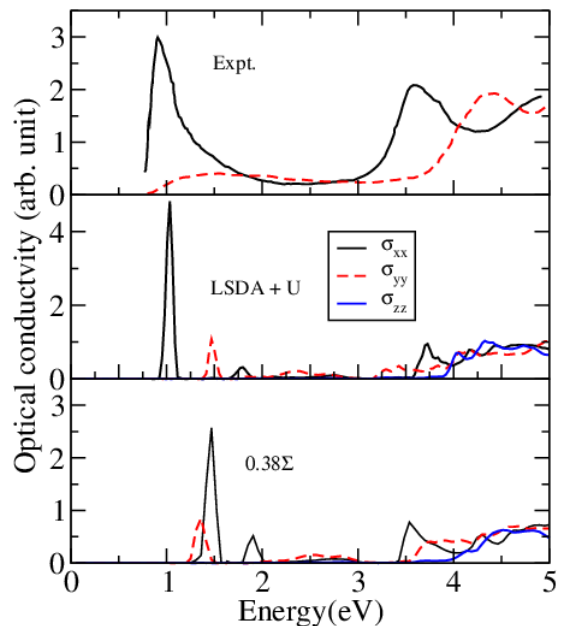


FIG. 6. (Color on-line) Optical conductivity of AFM1  $\text{NaV}_2\text{O}_5$ : top panel, experiment<sup>53</sup>; middle panel, LSDA+ $U$ ; and bottom panel,  $0.38\Delta\Sigma$ .

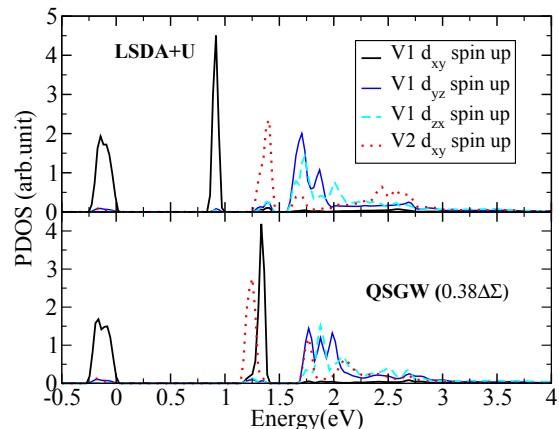


FIG. 7. (Color-on-line) PDOS on V atoms in the filled and empty split-off bands and low conduction bands relevant to the optical transitions obtained top panel in LSDA+ $U$  with  $U = 2.72$  eV and bottom panel in QSGW  $0.38\Delta\Sigma$ .

to the V- $d_{xy}$  derived which forms anti-bonding interactions with  $\text{O}_{\text{bridge-}p_y}$ . In previous work this is sometimes called the anti-bonding  $xy$  band.

In a simple tight-binding model, the “molecular” states of the rung, from which the split-off bands are constructed can be described by a Hamiltonian of the form

$$H = \begin{pmatrix} E_d & & V_{dp\pi} \\ & E_d & V_{dp\pi} \\ V_{dp\pi} & V_{dp\pi} & E_p \end{pmatrix} \quad (2)$$

The basis functions here correspond to  $d_{xy}^1$  on the left V atom,  $d_{xy}^2$  on the right V atom, and  $p_y$  on the bridge oxygen between them. There is only a  $V_{dp\pi}$  interaction between the O and V orbitals. One may now down-fold the  $p$ -states into the  $d$ -states to obtain an effective  $2 \times 2$  Hamiltonian:

$$H_{VV} = \begin{pmatrix} E_d + \frac{V_{dp\pi}^2}{E_d - E_p} & \frac{V_{dp\pi}^2}{E_d - E_p} \\ \frac{V_{dp\pi}^2}{E_d - E_p} & E_d + \frac{V_{dp\pi}^2}{E_d - E_p} \end{pmatrix} \quad (3)$$

whose eigenvalues finally are:

$$\begin{aligned} E_b &= E_d, \\ E_a &= E_d + 2 \frac{V_{dp\pi}^2}{E_d - E_p} \end{aligned} \quad (4)$$

In other words, for the symmetric or bonding combination of the two effective  $d$ -orbitals, the anti-bonding interactions with O- $p$  canceled out. In fact, by symmetry one can see easily that if the two  $xy$  orbitals have the same sign, they are antisymmetric with respect to the mirror plane passing through the bridge and therefore do not interact with the O- $p_y$ . The antisymmetric or anti-bonding combination however has twice the anti-bonding interaction with O- $p_y$ . From this it becomes clear that for polarization  $\mathbf{E} \parallel \mathbf{a}$  which is also antisymmetric with respect to this mirror plane, optical transitions are allowed between these bonding and anti-bonding  $xy$  orbital combinations on the same rung. Apparently, our  $0.38\Delta\Sigma$  model slightly overestimates this bonding to anti-bonding gap, just as it still slightly overestimates the O-2 $p$  - V- $d$  gap. This may be because we do not yet fully accurately include the anisotropies of the lattice polarization effect, and/or because of missing electron-hole interaction effects on the screened Coulomb interaction  $W$ . The assignment of this peak for  $\mathbf{E} \parallel \mathbf{a}$  agrees with that by Atzkern *et al.*<sup>53</sup>.

This transition is not allowed for  $\mathbf{E} \parallel \mathbf{b}$  for the symmetry reasons explained above, but we find a weaker transition, which in LSDA+ $U$  occurs at slightly higher energy and in  $0.38\Delta\Sigma$  occurs slightly below it. Further inspection shows that in LSDA+ $U$ , the first narrow set of empty  $d$ -bands again split in two, while in  $0.38\Delta\Sigma$ , they are closer together. Inspecting the PDOS shows that the band corresponding to this transition has opposite spin character to the occupied  $d$  band which is the initial state of the transition. In fact, Atzkern *et al.*<sup>53</sup> assigned this transition to a  $d_{xy} \uparrow$  to  $d_{xy} \downarrow$  transition. However, without circularly polarized light, there should not be transitions between up and down spin. However, because of the anti-ferromagnetic order along the  $\mathbf{b}$  axis, or the chain, it means that the atoms along the chain have alternating spin. So, this is in fact a transition from one V to the next V along the chain between states with the same spin. It is now clear why this transition becomes allowed for  $\mathbf{E} \parallel \mathbf{b}$ .

This transition is indeed seen as a much weaker peak in Fig.3 of Ref.52 for  $\mathbf{E} \parallel \mathbf{b}$  or also in Atzkern *et al.*<sup>53</sup> reproduced here as the upper panel in Fig.6. The fact

TABLE II. Band gaps and other energy differences in NaV<sub>2</sub>O<sub>5</sub>.  $\Delta_x$  is the spin-splitting of the FM split-off band,  $E_{gd}$  is the lowest direct gap between occupied  $d$  and empty  $d$  states,  $E_{gpd}$  is the lowest direct gap between O-2 $p$  like VBM and empty  $d$  states.  $W_d$  is the width of the split off majority spin band,  $E_{d1}$  is the gap between occupied  $d_{xy}$  and empty anti-bonding  $d_{xy}$  bands;  $E_{d2}$  is the gap between occupied  $d_{xy} \uparrow$  and  $d_{xy} \downarrow$  on the same atom,  $E_a$  and  $E_b$  are the transitions from the O-2 $p$  VBM to the same final states. The calculated transitions are indicated in the band figures. The corresponding experimental features  $E_{d1}$ ,  $E_a$  and  $E_{d2}$ ,  $E_b$  correspond to peaks for  $\mathbf{E} \parallel \mathbf{a}$  and  $\mathbf{E} \parallel \mathbf{b}$  respectively. All energies are in eV.

method	FM				AFM			
	$\Delta_x$	$E_{gd}$	$E_{gpd}$	$W_d$	$E_{d1}$	$E_{d2}$	$E_a$	$E_b$
QSGW	2.96	1.97	5.21	0.91	1.90	1.81	4.97	4.83
$0.38\Delta\Sigma$	1.68	1	3.5	0.91	1.36	1.14	3.72	3.50
$0.5\Delta\Sigma$	1.93	1.25	3.76	0.92	1.40	1.22	3.89	3.69
LSDA+ $U^a$	1.66	0.48	3.10	0.86	0.92	1.32	3.26	3.74
LSDA					0.48	0.84	3.25	3.62
Expt. <sup>b</sup>					0.9	1.2	3.25	3.9

<sup>a</sup>  $U = 2.72$  eV

<sup>b</sup> From Ref. 52

that this is an optical transition involving charge transfer from one rung to the next in the ladder explains why it is weaker in oscillator strength than the  $\mathbf{E} \parallel \mathbf{a}$  transition which is between molecular states localized on the same rung.

Since this transition is essentially resulting from the spin-splitting of the  $d$  band, it is sensitive to the  $U$  value chosen, as was found by Atzkern *et al.*<sup>53</sup>. We find this transition at about the same energy in LSDA+ $U$  with  $U_{\text{eff}} = 2.72$  and in  $0.38\Delta\Sigma$ , which again justifies the choice of  $U_{\text{eff}}$ -value. The  $\mathbf{E} \parallel \mathbf{a}$  transition on the other hand was found to be rather independent of  $U$  because it results from the bonding to anti-bonding splitting of the  $xy$  bands instead.

At higher energy near 3.5 eV for  $\mathbf{E} \parallel \mathbf{a}$  and 4.0 eV for  $\mathbf{E} \parallel \mathbf{b}$  we observe the transitions from the O-2 $p$  valence band maximum to these same two bands. We labeled these  $E_a$ ,  $E_b$  and they are listed in the Table II. These peaks are broader and probably also include transitions to the higher-lying  $d_{xz}$  and  $d_{yz}$  orbitals near the bottom of conduction band continuum. In between the two lowest peaks and the 3.5 eV and beyond ones, we see some small peaks in our calculations which correspond to the onset of transitions from the occupied  $d_{xy}$  band to the continuum of  $d$ -bands which is dominated by  $d_{xz}$  and  $d_{yz}$  like states. A background of transitions is also visible in the experiments. The experimental first peak shows a marked asymmetric broadening. Atzkern *et al.*<sup>53</sup> attempted to explain this in terms of spin-wave fluctuations away from the perfect anti-ferromagnetic ordering. They considered spiral spin waves which indeed broaden the majority spin occupied split-off  $d$ -band. However, they were still not able to fully account for the line shape

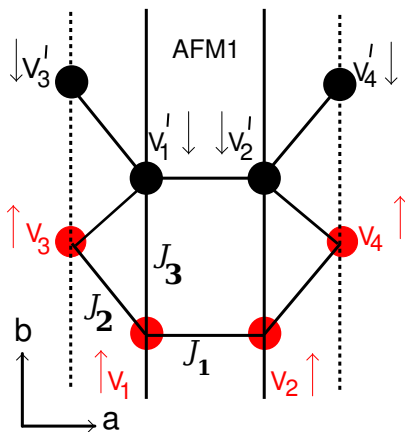


FIG. 8. (Color on-line) AFM1 spin configuration and labeling of the V atoms.  $V_1 - V_2$  form the central rung connected by a bridge oxygen. In the AFM1 model, the  $V_{1-4}$  atoms (red) have opposite spin of the  $V'_{1-4}$  atoms. The exchange interactions are indicated.

of this peak.

In Kontantinovič et al.'s work<sup>52</sup> additional features are seen in the optical conductivity, which were interpreted as transitions to an impurity band in between the lowest empty  $d$  and filled  $d$  bands. This impurity band occurs only when the Na concentration is less than 100 %. However, the new empty split-off band in the anti-ferromagnetic case which we here interpreted as the opposite spin counterpart to the bonding  $xy$  band, was not identified before. Finally, we summarize the band gaps and splittings in  $\text{NaV}_2\text{O}_5$  obtained in different approximations in Table II for both the FM and AFM case. Even though the FM is not found to occur experimentally, it is important because potentially it could be realized by placing the sample in a saturating magnetic field and may occur for significantly lower Na concentrations as we will discuss below.

### 5. Anti-ferromagnetic ordering and exchange couplings

Now, we address the total energy differences between different magnetic configurations and the exchange interactions. These were calculated within the LSDA+ $U$  approach with  $U_{\text{eff}} = 2.72$  eV. First, in Fig. 8 we show the experimentally occurring AFM structure, which we label as AFM1. We number the V-atoms 1-4 and 1'-4' as indicated to identify the other spin configurations considered in Table III.

These energy differences can be described by a generalized Heisenberg Hamiltonian of the form

$$H = - \sum_{i \neq j} J_{ij} \mathbf{e}_i \cdot \mathbf{e}_j \quad (5)$$

where the sum is over both  $i$  and  $j$ , so it counts each neighbor pair twice and the spins are represented as classical unit vectors. This means the magnetic moments

TABLE III. Total energies of different magnetic configurations relative to the ground state. The V atoms in the  $1 \times 2 \times 1$  cell are labeled in Fig. 8.

	1	2	3	4	1'	2'	3'	4'	$\Delta E$ (meV)
NM									160
FM	↑	↑	↑	↑	↑	↑	↑	↑	139
AFM1	↑	↑	↑	↑	↓	↓	↓	↓	0
AFM2	↑	↓	↑	↓	↓	↑	↓	↑	717
AFM3	↑	↓	↓	↑	↑	↓	↓	↑	713
AFM4	↑	↑	↓	↓	↓	↓	↑	↑	4

are folded into the definition of the  $J_{ij}$ . The magnetic moments here are found to be about  $0.5 \mu_B/V$  for AFM, which indicates single electron occupation per rung or V-pair. The net moments are found to be slightly larger in the FM than in the AFM case. We include the exchange interactions  $J_1$  with  $n = 1, 2, 3$  as follows:  $J_1$  is between  $V_1$  and  $V_2$ ,  $J_2$  between  $V_1$  and  $V_3$ , and  $J_3$  between  $V_1$  and  $V_1'$ . The total energies of the 8 V-atom cell of each of the configurations are then given by

$$\begin{aligned} E(FM) &= -8J_1 - 16J_2 - 16J_3, \\ E(AF1) &= -8J_1 + 16J_3, \\ E(AF2) &= 8J_1 + 16J_3, \\ E(AF3) &= 8J_1 + 16J_2 - 16J_3, \\ E(AF4) &= -8J_1 + 16J_3 \end{aligned} \quad (6)$$

We see that within the model up to 3rd neighbor interactions AFM4 and AFM1 have the same energy. In our calculations they differ by only 4 meV. Even if one would include a  $J_4$  between  $V_1$  and  $V_4$ , they would still be equal. So they differ only by some further range interaction. Within this model, we can extract 3 energy differences and hence the 3 exchange parameters.

We see immediately that  $E(AF2) - E(AF1) = 16J_1$  and hence  $J_1$  is 44.8 meV. This indicates a strong ferromagnetic coupling between the two V in the same rung. This is not surprising. In fact, if one thinks of the half-filled ladder as only having one electron in each rung spread over the two V atoms, then obviously, they must have the same spin. On the other hand, we readily find  $J_2 = -4.5$  meV and  $J_3 = -2.1$  meV. Thus both of these interactions are anti-ferromagnetic and they fall off as function of distance. It indicates that the neighboring chains want to be anti-ferromagnetically coupled as well as the ordering inside the chain tends to be anti-ferromagnetic. The last conclusion agrees with the study by Atzkern *et al.*<sup>53</sup>. These authors started from the AFM1 observed structure and within LSDA+ $U$  extracted exchange interactions from the spin-wave excitations.

The anti-ferromagnetic interaction  $J_3$  between atoms along the chain can be thought of as super-exchange via the chain oxygens connecting the V-atoms. More precisely they interact via the  $pd\pi$  interaction with  $\text{O}^{\text{chain}} - p_x$ . We obtain a super-exchange interaction here, because

the bonding  $xy$ -band of each spin is exactly filled. On the other hand, the exchange interaction  $J_2$  between adjacent ladders cannot be mediated by indirect super-exchange because  $V_3$ -O<sup>chain</sup>- $V_1$  form close to a right angle, and thus the electron could for example hop from  $V_1$  to a O- $p_y$  but then this  $y$  orbital is orthogonal to the  $xy$  on the  $V_3$ . However, these two V are close enough to have a direct exchange interaction. If they have sufficient overlap than the simple Heitler-London picture would predict the interaction to be anti-ferromagnetic as we indeed find to be the case. With this identification of the type of exchange interactions, we may expect that if we dope the band with fewer electrons, then, at some point, the indirect super-exchange will switch to ferromagnetic double exchange along the chain based on the Anderson-Hasegawa model.<sup>55</sup> In a later section (Sec. III C 2), we will determine the critical doping level where this crossover to ferro-magnetism occurs. The above analysis of the nature of the exchange interactions is similar to that by Horsch and Mack.<sup>56</sup>

We may further compare our exchange interactions with previous work in literature. For example, Fan *et al.*<sup>57</sup> reported  $J_{\parallel}$ , which is our  $J_3$  to be  $-51.1$  meV or  $-593$  K. However, they considered a  $S = 1/2$  spin-Hamiltonian instead of a classical unit-vector spin Hamiltonian so due to this different normalization our values are a factor four smaller. Furthermore they counted each pair only once, whereas our definition of the spin-Hamiltonian counts each pair twice. In fact, their energy difference  $E(FM) - E(AFM) = 25$  meV per formula unit, *i.e.* per V-pair. This means 100 meV per 8 atom cell, compared to our 139 meV. The difference however is that we attribute this in part to the exchange interactions in adjacent chains, which is present in the ferromagnetic case but cancels in the anti-ferromagnetic case, whereas they attribute it solely to the interactions between V in the single ladder. Our FM-AFM energy difference per pair of V atoms, or per formula unit is 34.75 meV or 403 K. Our value for the parameter  $J_{\parallel}$  as reported by Fan *et al.*<sup>57</sup> would be  $-806$  K. In fact, in literature, values between  $-529$  K and  $-928$  K were reported for this parameter in de Graaf *et al.*<sup>58</sup> based on various computational estimates and experimental values. References to the rest of the literature on exchange interactions in  $\text{NaV}_2\text{O}_5$  can be found there.

### C. Band structure of $\text{V}_2\text{O}_5$ doped by carrier injection

In this section, we try different alternative ways of doping  $\text{V}_2\text{O}_5$  compared with  $\text{NaV}_2\text{O}_5$ . Our goal here is twofold. First, we want to explore how different or similar the resulting band structures are to those of  $\text{NaV}_2\text{O}_5$ . Secondly, we want to view these as simulating doping by gating and determine which approach most closely achieves this and could be used to simulate continuous variation of the electron concentrations ranging from

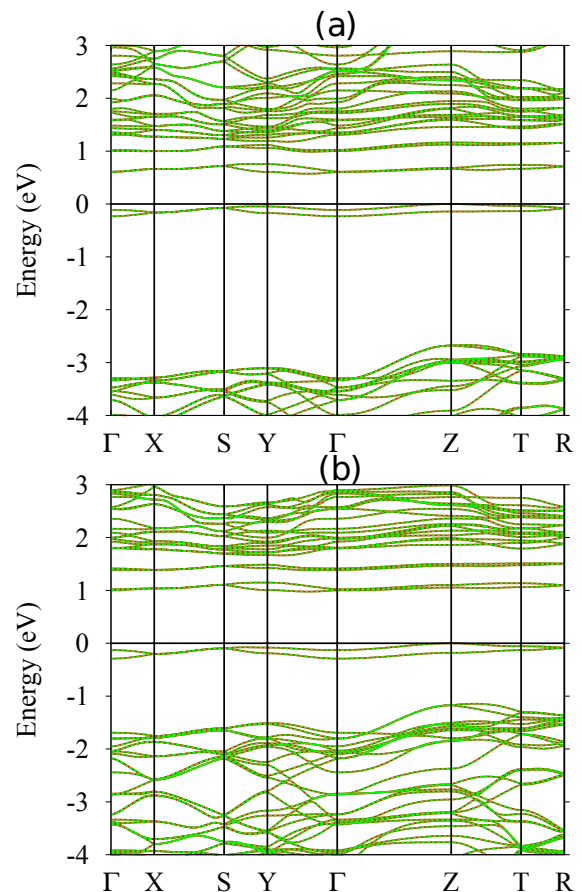


FIG. 9. (Color on-line) Band structures of AFM doped  $\text{V}_2\text{O}_5$  with (a) homogeneous background  $QB = 2$  in upper figure and (b) VCA by using V with  $Z = 23.5$ . Both are obtained within QSGW with  $0.38\Delta\Sigma$ .

$0 < x < 1$  in the bonding  $xy$ -band.

#### 1. Background vs. Virtual crystal approximation

First we keep the filling of the band the same as in  $\text{NaV}_2\text{O}_5$ . That is 2 electrons are added per unit cell or 1 per  $\text{V}_2\text{O}_5$  unit, or 1 electron per rung in the ladder in the  $xy$ -bonding band. The first approach is to compensate the 2 electrons by a uniform positive background  $QB = 2$ . The second approach we consider is to compensate the electronic charge by spreading it over the vanadium nuclei. We call this the virtual crystal approximation (VCA). It means we replace the atomic number of V by  $Z = 23.5$ . In Fig. 9 we show the band structures in the  $0.38\Delta\Sigma$  model for the background and for the VCA for the AFM ordered case. These should be compared with the corresponding  $\text{NaV}_2\text{O}_5$  case in Fig. 4.

We can see that the splitting between the occupied  $d$  band and the oxygen VBM reduces from the  $QB = 2$  to  $\text{NaV}_2\text{O}_5$  to the VCA case. This can be explained from the differences in electrostatic potential. In the VCA case, we place the compensating positive charge on the

TABLE IV. Oxygen  $p$  to vanadium  $d_{xy}$  band energy difference (eV) in different doping models with QSGW  $0.38\Delta\Sigma$ .

VCA	NaV <sub>2</sub> O <sub>5</sub>	$QB = 2$
1.00	2.02	2.53

vanadium very close to where the electrons in this band are localized. So, the electrons feel a stronger attractive potential, pulling this band down. In the NaV<sub>2</sub>O<sub>5</sub> case, the compensating positive charge is residing on the Na<sup>+</sup> ions in the interstitial region between the layers. Compared to the VCA, clearly the attractive potential will be weaker. Finally, if we spread the positive charge out homogeneously in a background, the electrostatic interaction is even weaker, even though some of the charge now resides in the V<sub>2</sub>O<sub>5</sub> layer and some in the interstitial, both are smeared out. The same trend is observed in the ferromagnetic band structures. Also similar results are found for our LSDA+ $U$  model.

We also examined how these different models affect the magnetic ordering. We focus here only on the ordering of moments along the chain. We find that in the background model, the ordering is still anti-ferromagnetic but in the VCA case it becomes ferromagnetic or very close to equal energy for ferromagnetic and anti-ferromagnetic ordering.

Finally, we should note that in the background and VCA models, we used the original V<sub>2</sub>O<sub>5</sub> structure which differs slightly from the NaV<sub>2</sub>O<sub>5</sub> structure. The  $\mathbf{c}$  lattice constant is somewhat smaller and the pyramids around vanadium are not rotated toward the Na interstitial site. This leads to a slightly smaller band width of the filled split-off band in the ferromagnetic case.

From all this, we conclude that the background model seems more appropriate than the VCA in which compensating charge is placed right on the layer in the V atoms because the latter would yield incorrect predictions about the magnetic order. If we think about a model for injecting charge from a gate, the latter could consist for example of a metallic layer above and below the atomically thin V<sub>2</sub>O<sub>5</sub> film. This means the opposite positive charge should stay away from the layer. The background model somewhat achieve this but not quite as accurately as Na itself. In the next section we therefore consider applying the VCA to Na instead. If we replace  $Z=11$  of Na by  $Z = 11 - x$ , we simulate in some sense a reduced concentration of Na atoms, we could think about it as replacing some of the Na by inert Ne atoms with  $Z = 10$ . This could also be viewed as a model for a metallic layer which injects charge into V<sub>2</sub>O<sub>5</sub>.

## 2. Continuous doping models

In this section, we present results for  $QB$  doping with  $QB = 1$  and  $0.5$  and also calculations with a VCA for Na atoms with  $Z$  continuously varying from 10 to 11.

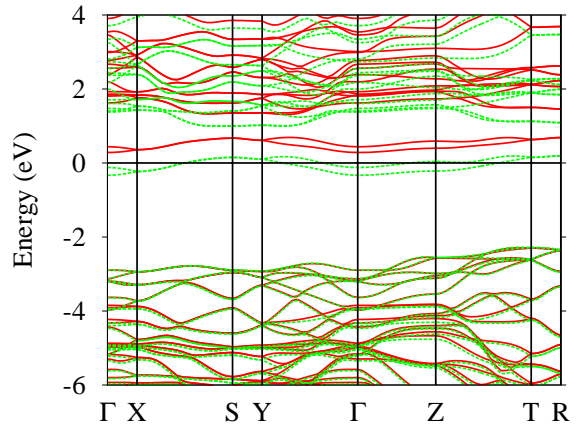


FIG. 10. (Color-on-line) Band structure of background doped V<sub>2</sub>O<sub>5</sub> for  $QB = 1$ , which is ferromagnetic in QSGW with  $0.38\Delta\Sigma$ .

For  $QB = 1$  as shown in Fig. 10 we find as expected a ferromagnetic metallic band structure, with the partially filled band fairly close (about 1 eV) from the CBM. The distance to the VBM depends as before on whether we use LSDA, LSDA+ $U$ , QSGW or  $0.38\Delta\Sigma$  QSGW + lattice polarization effect. The exchange splitting  $\Delta_x$  is smaller in LSDA than in  $GW$  and is also reduced further if we reduce the background charge to 0.5 (not shown). The exchange splitting  $\Delta_x$  varies from 1.07 to 0.59 to 0.21 eV for  $QB = 2, 1, 0.5$  respectively. Anti-ferromagnetic structures are less stable in this case. So, this already predicts that for small filling of the band ferromagnetic moments could occur but there might be a minimum filling required before the exchange splitting  $\Delta_x$  is sufficiently large to keep the two bands separate and the half-metallic character preserved. For too small doping, we might simply revert to a non-magnetic filling of the band.

On the other hand, we are interested also in the case of nearly filled doping, as could occur for example in slightly under-doping with Na, or in the case of Na doping but extracting some electrons out of the layer by gating. In that case, we would start from an AFM ordering along the chains but could locally convert it to FM ordering if we achieve a critical reduction in carrier concentration in the band. This we study by means of NaV<sub>2</sub>O<sub>5</sub> with  $10 \leq Z_{\text{Na}} \leq 11$  VCA. The magnetic moment of vanadium (shown in Fig.11c) approaches zero for  $Z_{\text{Na}} \rightarrow 10$ . This would indicate ferromagnetic ordering even for very small doping of the band. The width of split-off band ( $\Delta_x$  also varies almost linearly with  $Z_{\text{Na}}$  going from 11 to 10 as shown in Fig.11b. However, in reality instead of having a very small spread-out itinerant moment, one might expect localized moments too far from each other to interact. There would thus be some kind of percola-

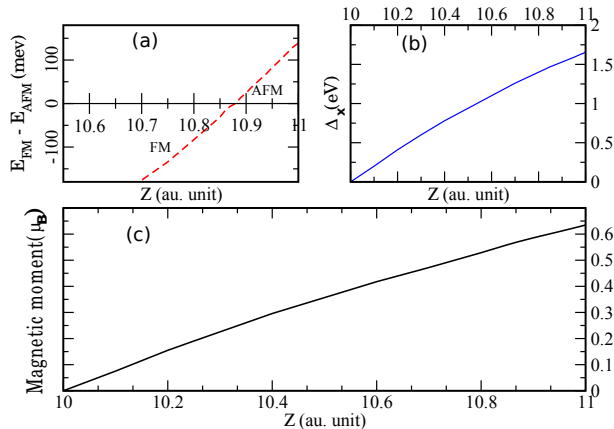


FIG. 11. (Color on-line) a) Variation of energy difference  $E_{FM} - E_{AFM}$  b) split-off band width  $\Delta_x$  and c) magnetic moment per vanadium atom as a function of  $Z$  respectively.

tion cut-off and one might expect  $\text{Na}_x\text{V}_2\text{O}_5$  for small  $x$  to be paramagnetic instead of ferromagnetic. This is indeed found to be the case for  $\text{Na}_{0.33}\text{V}_2\text{O}_5$  in Chakraverty *et al.*<sup>59</sup> On the other hand, there is a crossover between the two competing magnetically ordered states (AFM1 and FM) at  $Z = 10.88$ . This is shown in Fig.11a. The band structure becomes metallic for carrier concentration between 0.9 and 1.0 in the split-off  $d_{xy}$  bonding band even though the system is anti-ferromagnetically ordered. This is shown in Fig. 12 which shows a close up of the bands near the Fermi energy. One can see a slight splitting of the up and down spin bands, which also results in a slightly different up and down magnetic moment. This indicates already some gradual transition to the ferromagnetic configuration. Strictly speaking this system is found to be ferrimagnetic in our calculation but the changes in moment are close to the numerical uncertainty of the self-consistent calculation.

#### IV. CONCLUSIONS

In this paper we studied doping of the  $\text{V}_2\text{O}_5$  split-off conduction band, first by means of intercalation with Na as in the bronze  $\text{NaV}_2\text{O}_5$  using first-principles calculations. We found that the half-filling leads to a spin-splitting of this band of about 2 eV within the QSGW method or QSGW method with lattice-polarization correction, as applied previously to pure  $\text{V}_2\text{O}_5$ . This agrees well with the results of LSDA+ $U$  with  $U_{\text{eff}} \approx 2.7$  eV. This further induces spin-splittings of the higher lying conduction bands. This corresponds to a magnetic moment of  $1\mu_B$  per  $\text{V} - \text{O}^{\text{bridge}} - \text{V}$  rung. These moments are found to order anti-ferromagnetically along the chain and of course, the effective moments of  $0.5\mu_B$  on the V atoms on

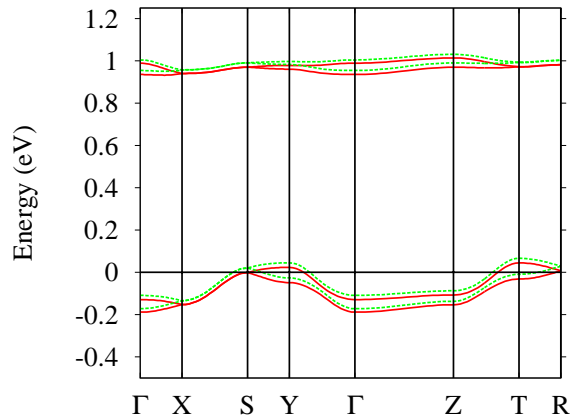


FIG. 12. (Color on-line) Band structure of metallic  $\text{Na}_{0.9}\text{V}_2\text{O}_5$  AFM calculated in LSDA+ $U$ .

the same rung are found to prefer strongly to be parallel. However, the staggered neighboring chains or ladders are also found to order anti-ferromagnetically. The exchange interaction between V atoms along the chain is found to be smaller than the exchange interaction between V in the adjacent chains. The former is an anti-ferromagnetic super-exchange while the latter is a direct V-V interaction. Both contribute to the energy difference from the ferromagnetic state. The FM-AFM energy difference per formula unit is found to be within the range of values previously reported in literature by both experimental determinations and other computations. However, our analysis of the intra-chain and inter-chain exchange interactions differs from previous results, in which either the inter-chain interaction is neglected or found to be ferromagnetic. Our exchange interactions were extracted from comparing various spin configurations within the LSDA+ $U$  model with the  $U_{\text{eff}}$  value justified by both agreement with the parameter-free QSGW method and optical experiments on the AFM model.

The band structure in the anti-ferromagnetic ground state is found to have much smaller band widths of the split-off bands, which is explained by the fact that in the AFM case, hopping between nearest neighbors along the chain is prohibited because they have opposite spin. Above the filled band, new states split-off from the continuum. One of these is the anti-bonding  $d_{xy}$  band and the other is the opposite spin counter-part of the bonding  $d_{xy}$  band. Both actually result in two bands because of the two chains per unit cell. Optical transitions between the filled  $d_{xy}$  band to these empty split-off bands result in two closely spaced peaks in optical conductivity for  $\mathbf{E} \parallel \mathbf{a}$  polarization and  $\mathbf{E} \parallel \mathbf{b}$ . The former correspond to transitions between bonding and anti-bonding  $d_{xy}$  combinations on the same rung, while the latter corresponds to a transition between the spin-split bands which have both

bonding character. More precisely, the latter should be viewed as transitions between alternating V-atoms along the chain with the same spin. The latter are therefore weaker than the transitions within the same rung. Optical transitions from O-2*p* valence bands to these same final empty states are found correspondingly at slightly higher energy for  $\mathbf{E} \parallel \mathbf{b}$  than for  $\mathbf{E} \parallel \mathbf{a}$ . These interpretations of the optical transitions agree closely with previous work in literature. We found that the QSGW method slightly overestimates the bonding-anti-bonding transition but gives a good value for the spin-splitting  $\Delta_x$ .

Various ways for simulating doping by carriers without adding Na explicitly were studied. We found that the position of the occupied split-off band depends strongly on how the electron doping is compensated. This is explained in terms of the different electrostatics. For example, a homogeneous background provides a less attractive electrostatic potential than  $\text{Na}^+$  ions in the interstitial space between the layers, or than placing the counter charge on the V atoms. The splitting between bonding and anti-bonding  $d_{xy}$  orbitals or spin-splitting however remains the same as before and is independent of this choice of compensating charge. From the point of view of simulating doping by gating, the compensating charge should be kept away from the doped layer. This is in fact best achieved by Na atoms in the interstitial. One might view the latter as a metallic contact layer. In order to simulate continuously varying electron doping, we then proposed a virtual crystal approximation treatment in which the atomic number  $Z_{\text{Na}}$  is varied between 10 and 11, 10 representing inert Ne atoms. This model can then simulate both a reduced Na concentration intercalation or a metallic contact gate which pushes a carrier concentration into the  $\text{V}_2\text{O}_5$  layer that can be tuned continuously between 0 and 2 per unit cell or 0 and 1 per  $\text{V}_2\text{O}_5$  formula unit, which is equivalent to one ladder. Within this model, we found that for carrier concentrations less than 0.88 *e*/formula unit, the ordering of the moments switches from AFM to FM. This is in fact expected on the basis of the Anderson-Hasegawa model where the exchange interactions would switch from AFM

super-exchange to ferro-magnetic double exchange. The same model predicts FM ordering but with continuously decreasing moments all the way down to zero carrier concentration. However, the latter is unrealistic. One should instead expect that there is a minimum critical concentration before localized moments in the chain reach a percolation threshold. In the present model these moments behave like an itinerant ferromagnet which loses its moments only when zero concentration is reached.

To a large extent our results confirm previous analysis for  $\text{NaV}_2\text{O}_5$ . However, we emphasize the new perspective that in atomically thin layers alternate approaches than variations in the Na concentration could be used to control the charge and thus induce a change from AFM to FM ordering. With the accessibility of the surface to local probes such as an STM tip, this might lead to the control of the local spin alignment on an atomic scale. We caution however, that further complicating issues should be considered here, such as the spin-Peierls or charge ordering transition occurring at low temperatures, the imperfect ordering in one-dimension accompanied by spin-wave excitation fluctuations at finite temperature, etc. Still, our final conclusion is that this system provides possibly an intriguing playground for manipulating spins on the atomic scale at surfaces.

## ACKNOWLEDGMENTS

This work was supported by the Air Force Office of Scientific Research under Grant number FA 9550-12-1-0441 (CB) and the US Department of Energy, Office of Science, Basic Energy Sciences, under grant No. ER-46874-SC0008933 (WL). The strongly correlated  $\text{NaV}_2\text{O}_5$  aspects of the work and investigation of the QSGW methodology to new systems were supported by DOE while the complex 2D oxide electronics aspects were supported by AFOSR. The calculations were performed at the High Performance Computing Resource in the Core Facility for Advanced Research Computing at Case Western Reserve University.

<sup>1</sup> C. Bhandari, W. R. L. Lambrecht, and M. van Schilf-gaarde, *Phys. Rev. B* **91**, 125116 (2015).

<sup>2</sup> H. Smolinski, C. Gros, W. Weber, U. Peuchert, G. Roth, M. Weiden, and C. Geibel, *Phys. Rev. Lett.* **80**, 5164 (1998).

<sup>3</sup> W. Lambrecht, B. Djafari-Rouahni, and J. Vennik, *J. Phys.C: Solid State Phys.* **14** (1981).

<sup>4</sup> G. Bauer, V. Güther, H. Hess, A. Otto, O. Roidl, H. Roller, and S. Sattelberger, "Vanadium and Vanadium Compounds," in *Ullmann's Encyclopedia of Industrial Chemistry* (Wiley-VCH, Weinheim, 2005).

<sup>5</sup> M. Ponzi, C. Duschatzky, A. Carrascull, and E. Ponzi, *Applied Catalysis A: General* **169**, 373 (1998).

<sup>6</sup> A.-M. Cao, J.-S. Hu, H.-P. Liang, and L.-J. Wan, *Angewandte Chemie International Edition* **44**, 4391 (2005).

<sup>7</sup> C. Wu and Y. Xie, *Energy Environ. Sci.* **3**, 1191 (2010).

<sup>8</sup> S. F. Cogan, N. M. Nguyen, S. J. Perrotti, and R. D. Rauh (1989) pp. 57–62.

<sup>9</sup> G. Nadkarni and V. Shirodkar, *Thin Solid Films* **105**, 115 (1983).

<sup>10</sup> Z. R. Xiao, G. Y. Guo, P. H. Lee, H. S. Hsu, and J. C. A. Huang, *Journal of the Physical Society of Japan* **77**, 023706 (2008), <http://dx.doi.org/10.1143/JPSJ.77.023706>.

<sup>11</sup> M. Isobe and Y. Ueda, *J. Phys. Soc. Jpn.* **65**, 1178 (1996).

<sup>12</sup> C. Haas, *Phys. Rev.* **125**, 1965 (1962).

<sup>13</sup> E. O. Kane, *Phys. Rev.* **131**, 79 (1963).

<sup>14</sup> K. F. Berggren and B. E. Sernelius, *Phys. Rev. B* **24**, 1971 (1981).

- <sup>15</sup> T. S. Moss, Proceedings of the Physical Society. Section B **67**, 775 (1954).
- <sup>16</sup> E. Burstein, Phys. Rev. **93**, 632 (1954).
- <sup>17</sup> Y. Ueda and M. Isobe, Journal of Magnetism and Magnetic Materials **177181**, Part 1, 741 (1998), international Conference on Magnetism.
- <sup>18</sup> W. Mumme and J. Watts, Journal of Solid State Chemistry **3**, 319 (1971).
- <sup>19</sup> Y. Kanke, K. Kato, E. Takayama-Muromachi, and M. Isobe, Acta Crystallographica Section C **46**, 536 (1990).
- <sup>20</sup> A. Casalot, D. Lavaud, J. Galy, and P. Hagenmuller, Journal of Solid State Chemistry **2**, 544 (1970).
- <sup>21</sup> S. Anderson, Acta. Chem. Scand. , 1361 (1965).
- <sup>22</sup> A. Carpy, A. Casalot, M. Pouchard, J. Galy, and P. Hagenmuller, Journal of Solid State Chemistry **5**, 229 (1972).
- <sup>23</sup> I. S. Jacobs, J. W. Bray, H. R. Hart, L. V. Interrante, J. S. Kasper, G. D. Watkins, D. E. Prober, and J. C. Bonner, Phys. Rev. B **14**, 3036 (1976).
- <sup>24</sup> J. C. Bonner and M. E. Fisher, Phys. Rev. **135**, A640 (1964).
- <sup>25</sup> L. N. Bulaevskii, Sov. Physics, JETP , 684 (1963).
- <sup>26</sup> F. D. M. Haldane, Phys. Rev. B **25**, 4925 (1982).
- <sup>27</sup> F. D. M. Haldane, Phys. Rev. Lett. **50**, 1153 (1983).
- <sup>28</sup> M. Hase, I. Terasaki, and K. Uchinokura, Phys. Rev. Lett. **70**, 3651 (1993).
- <sup>29</sup> A. Meetsma, J. L. De Boer, A. Damascelli, J. Jegoudez, A. Revcolevschi, and T. T. M. Palstra, Acta Crystallographica Section C **54**, 1558 (1998).
- <sup>30</sup> M. Mostovoy and D. Khomskii, Solid state communications **113**, 159 (1999).
- <sup>31</sup> P. Thalmeier and P. Fulde, Europhysics Letters **44**, 242 (1998).
- <sup>32</sup> J. Lüdecke, A. Jobst, S. van Smaalen, E. Morré, C. Geibel, and H.-G. Krane, Phys. Rev. Lett. **82**, 3633 (1999).
- <sup>33</sup> A. I. Smirnov, M. N. Popova, A. B. Sushkov, S. A. Golubchik, D. I. Khomskii, M. V. Mostovoy, A. N. Vasil'ev, M. Isobe, and Y. Ueda, Phys. Rev. B **59**, 14546 (1999).
- <sup>34</sup> N. Suaud and M.-B. Lepetit, Phys. Rev. Lett. **88**, 056405 (2002).
- <sup>35</sup> A. Bernert, P. Thalmeier, and P. Fulde, Phys. Rev. B **66**, 165108 (2002).
- <sup>36</sup> L. Hozoi, A. H. de Vries, A. B. van Oosten, R. Broer, J. Cabrero, and C. de Graaf, Phys. Rev. Lett. **89**, 076407 (2002).
- <sup>37</sup> D. O. Scanlon, A. Walsh, B. J. Morgan, and G. W. Watson, The Journal of Physical Chemistry C **112**, 9903 (2008), <http://dx.doi.org/10.1021/jp711334f>.
- <sup>38</sup> C. Bhandari and W. R. L. Lambrecht, Phys. Rev. B **89**, 045109 (2014).
- <sup>39</sup> M. Methfessel, M. van Schilfgaarde, and R. A. Casali, in *Electronic Structure and Physical Properties of Solids. The Use of the LMTO Method*, Lecture Notes in Physics, Vol. 535, edited by H. Dreyssé (Berlin Springer Verlag, 2000) p. 114.
- <sup>40</sup> T. Kotani and M. van Schilfgaarde, Phys. Rev. B **81**, 125117 (2010).
- <sup>41</sup> W. Kohn and L. J. Sham, Phys. Rev. **140**, A1133 (1965).
- <sup>42</sup> U. von Barth and L. Hedin, Journal of Physics C: Solid State Physics **5**, 1629 (1972).
- <sup>43</sup> <http://www.lmsuite.org>.
- <sup>44</sup> <https://github.com/tkotani/ecalj>.
- <sup>45</sup> M. van Schilfgaarde, T. Kotani, and S. Faleev, Phys. Rev. Lett. **96**, 226402 (2006).
- <sup>46</sup> M. van Schilfgaarde, T. Kotani, and S. V. Faleev, Phys. Rev. B **74**, 245125 (2006).
- <sup>47</sup> T. Kotani, M. van Schilfgaarde, and S. V. Faleev, Phys. Rev. B **76**, 165106 (2007).
- <sup>48</sup> R. Enjalbert and J. Galy, Acta Crystallographica Section C **42**, 1467 (1986).
- <sup>49</sup> J. F. Janak, Phys. Rev. B **16**, 255 (1977).
- <sup>50</sup> M. N. Popova, A. B. Sushkov, S. A. Golubchik, B. N. Mavrin, V. N. Denisov, B. Z. Malkin, A. I. Iskhakova, M. Isobe, and Y. Ueda, Soviet Journal of Experimental and Theoretical Physics **88**, 1186 (1999), <condmat/9807369>.
- <sup>51</sup> X. Ming, H.-G. Fan, Z.-F. Huang, F. Hu, C.-Z. Wang, and G. Chen, Journal of Physics: Condensed Matter **20**, 155203 (2008).
- <sup>52</sup> M. J. Konstantinović, Z. V. Popović, V. V. Moshchalkov, C. Presura, R. Gajić, M. Isobe, and Y. Ueda, Phys. Rev. B **65**, 245103 (2002).
- <sup>53</sup> S. Atzkern, M. Knupfer, M. S. Golden, J. Fink, A. N. Yaresko, V. N. Antonov, A. Hübsch, C. Waidacher, K. W. Becker, W. von der Linden, G. Obermeier, and S. Horn, Phys. Rev. B **63**, 165113 (2001).
- <sup>54</sup> C. Presura, D. van der Marel, A. Damascelli, and R. K. Kremer, Phys. Rev. B **61**, 15762 (2000).
- <sup>55</sup> P. W. Anderson and H. Hasegawa, Phys. Rev. **100**, 675 (1955).
- <sup>56</sup> P. Horsch and F. Mack, Eur. Phys. J. B **5**, 367 (1998).
- <sup>57</sup> H.-g. Fan, X. Ming, F. Hu, C.-z. Wang, Z.-f. Huang, and G. Chen, Chem. Res. Chinese Universities **25**, 243 (2009).
- <sup>58</sup> C. de Graaf, L. Hozoi, and R. Broer, The Journal of Chemical Physics **120**, 961 (2004).
- <sup>59</sup> B. K. Chakraverty, M. J. Sienko, and J. Bonnerot, Phys. Rev. B **17**, 3781 (1978).